Role of sublimation and riming on the precipitation distribution in the Kananaskis Valley, Alberta, Canada

Émilie Poirier[1], Julie M. Thériault[1], and Maud Leriche[1,2]

[1]Centre ESCER, Departement of Earth and Atmospheric Sciences, Université du Québec à Montréal, Montréal, Québec, Canada
[2]Laboratoire d'Aérologie, CNRS, Université Paul Sabatier, Toulouse, France

Correspondence: Julie M. Thériault (theriault.julie@uqam.ca)

Abstract.

The phase of precipitation and its distribution at the surface can affect water resources and the regional water cycle of a region. A field project was held in March-April 2015 on the eastern slope of the Canadian Rockies to document precipitation characteristics and associated atmospheric conditions. During the project, 60% of the particles documented were rimed, in
5 relatively warm and dry conditions. Rain-snow transitions also occurred aloft and at the surface in sub-saturated conditions. Solid precipitation falling through a saturated atmospheric layer with temperatures >0°C will start melting. In contrast, if the melting layer is sub-saturated, the solid precipitation undergoes sublimation, which increases the depth of the rain-snow transition. In this context, this study investigates the role of sublimation and riming on precipitation intensity and type reaching the surface in the Kananaskis Valley, Alberta, where the field campaign took place during March-April 2015. To address this, a
10 set of numerical simulations of an event of mixed precipitation observed at the surface was conducted. This event on 31 March 2015, was documented with a set of devices at the main observation site (Kananaskis Emergency Services, KES) including a precipitation gauge, disdrometer, and micro rain radar. Sensitivity experiments were performed to assess the impacts of temperature changes from sublimation and the role of the production of snow pellets (riming) aloft on the surface precipitation evolution. A warmer environment associated with no temperature changes from sublimation leads to a peak in the intensity
15 of snow pellets at the surface. When the formation of snow pellets is not considered, the maximum snowfall rate occurred at later times. Results suggest that unrimed snow reaching the surface is formed on the western flank and is advected eastward. In contrast, snow pellets would form aloft in the Kananaskis Valley. The cooling from sublimation and melting by rime particles increases the vertical shear near KES. Overall, this study illustrated that the presence of snow pellets influenced the surface evolution of precipitation type in the valley due to the horizontal transport of precipitation particles.

20 # 1 Introduction

The phase of precipitation can lead to major disasters such as the Calgary 2013 flooding event (Milrad et al., 2015; Liu et al., 2016). In this particular event, the heavy rain generated rainfall runoff at low and mid elevations, but it was supplemented by rain-on-snow runoff at high elevations due to a late lying snowpack (Pomeroy et al., 2016). The rain-on-snow caused by a higher than usual rain-snow boundary was one of the many factors that led to this catastrophic flooding.

The rain-snow boundary, also called the precipitation transition region, is the area characterized by mixed precipitation bounded by only rain and only snow at the surface and aloft, respectively. Marwitz (1983) and Marwitz (1987) studied these rain-snow transitions in mountainous areas using observations over the Sierra Nevada, USA. They observed that the height of the radar bright band, associated with the top of the precipitation transition region, decreased by 400-600 m while approaching the mountain barrier, corresponding to a lower 0°C isotherm near the barrier. Simulations were also used to study the lowering of the rain-snow boundary on a mountain windward slope (Minder et al., 2011). These simulations identified three physical mechanisms influencing the location of the rain-snow boundary along the mountainside. These are cooling by melting of solid particles, adiabatic cooling of rising air, and the distance associated with complete melting of solid precipitation.

In a saturated environment, diabatic cooling due to melting of solid precipitation falling in a warm layer (T>0°C) can lead to a change in the valley wind flow. This was observed in the Toce river valley in the Italian Alps during the Mesoscale Alpine Program (MAP, Steiner et al., 2003) and during the 2010 Vancouver Olympics in the Whistler area (Thériault et al., 2012, 2015). However, Zängl (2007) using numerical simulations, suggested that the cooling by melting of snow was of less importance in creating the down-valley flow for the same event because of the impact of cooling associated with sublimation.

Because solid precipitation melts only when the wet-bulb temperature is >0°C, it can reach the surface at relatively warm temperatures in a dry environment. For examples, a few studies reported solid precipitation at surface air temperature of 4-6°C (e.g. Matsuo et al., 1981; Harder and Pomeroy, 2013). Few studies addressing the effects of cooling by sublimation in winter storms exist, especially in mountainous regions. For instance, Clough and Franks (1991) examined the evaporative processes in frontal and stratiform precipitation. They showed that sublimation of ice particles was an efficient thermodynamic process. Parker and Thorpe (1995) studied the role of snow sublimation on frontogenesis and showed that the cross-frontal flows in the vicinity of the sublimation were strongly modified and a mesoscale downdraft was produced below the synoptic frontal surface. Barth and Parsons (1996) highlighted that sublimation of snow and rimed particles played an important role in the modelled evolution of a narrow cold-frontal rain band.

Few studies have examined precipitation features in northern Canada. Burford and Stewart (1998) suggested that sublimation was the main process responsible of relatively low precipitation amounts observed at Inuvik and Tuktoyaktuk (Northwest Territories). Furthermore, Stewart et al. (2004) examined precipitation events at Fort Simpson (Northwest Territories) and found that hydrometeors were mainly single crystals and aggregates. The absence of rimed particles could explain the low precipitation amounts as single crystals and aggregates are more likely to sublimate while falling to the surface. In contrast, precipitation types were characterized in Iqaluit (Nunavut) by Henson et al. (2011) and Fargey et al. (2014). They observed that rimed particles, aggregates, and snow pellets were very common even during light precipitation events. They suggested that the development of rimed and large particles increased their likelihood of reaching the surface through the drier sub-cloud layer.

In this context, to better understand the processes leading to surface precipitation on the lee side of the Canadian Rockies, a field campaign was held during March-April 2015 in the Kananaskis Valley, Alberta (Fig. 1). The goal of this field campaign was to document precipitation and associated weather conditions in that region (Thériault et al., 2018). Given the importance of precipitation phase in this area, there is a need to improve our understanding of the microphysical processes leading to rain-
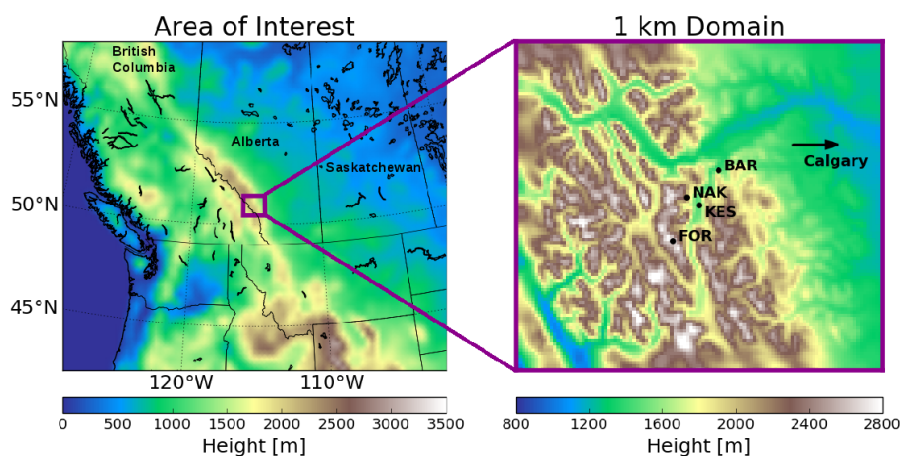
Figure 1. Area of interest and 1 km mesh domain used for the numerical simulations with the WRF model.

snow transition in this particular sub-saturated areas. The goal of this study is to investigate the role of sublimation and riming on the precipitation intensity and types reaching the surface in the Kananaskis Valley, Alberta. To address this, numerical simulations using the Weather Research Forecasting (WRF) model (Skamarock and Klemp, 2008) were conducted. A well-documented case study associated with mixed precipitation reaching the surface in the Kananaskis valley was chosen from the

5   2015 field campaign mentioned above.

    This paper is structured as follows. Section 2 provides an overview of the field project and describes the case study used in this paper. The methodology including, the model configuration, the sensitivity experiments and data analysis, is explained in Section 3. Results from the control simulation, the role of sublimation and the formation of rime snow are summarized in Section 4, 5 and 6, respectively. Finally, a summary and conclusion are given in Section 7.

10 **2   Overview of the case study**

During the field project held in the Kananaskis Valley during March-April 2015, a total of 17 precipitation events were documented Thériault et al. (2018) . These were associated with rain or snow only as well as mixture of precipitation. Solid precipitation was reported at the surface at temperatures up to 9°C but in very dry conditions (∼45% relative humidity), also noted by Harder and Pomeroy (2013), and most of them were rimed (∼60%).

15   Most of the observations were collected at the Kananaskis Emergency Services (KES) site located a few kilometers southeast of the Nakiska ski area (NAK) and about 15 km south of the Barrier Lake research station (BAR) (Fig. 1). Instrumentation used included a GEONOR precipitation gauge, a sounding system to measure vertical temperature and relative humidity profiles, a Parsivel optical disdrometer (Battaglia et al., 2010), and a Micro Rain Radar (MRR2). Basic meteorological measurements were also available (pressure, wind speed and direction, temperature, dew point temperature). Manual observations of weather

20 conditions were also reported in a systematic manner. Vertical profiles of basic meteorological features were also obtained using
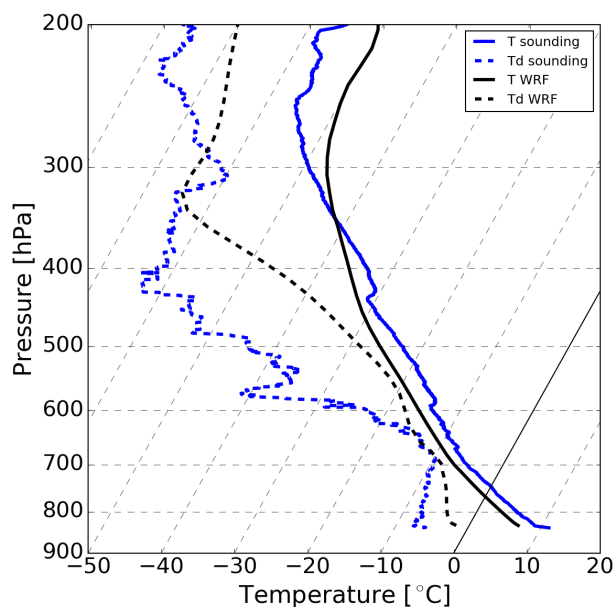
Figure 2. Vertical profiles of air temperature (solid line) and dew point temperature (dashed line) at 2100 UTC 31 March 2015 launched from the KES site from both measurements (blue lines) and the CTL simulation (black lines).

a Kestrel attached to a ski pole and a GPS (Thériault et al., 2014) at two other sites in the presence of rain-snow transitions at NAK and at Fortress Mountain (FOR). Further details about the field campaign are given in Thériault et al. (2018).

The well-documented weather event that occurred on 31 March 2015 was chosen for this study for three main reasons. First, all the weather instruments deployed at KES were operational. Second, a mixture of precipitation types and phase transition in sub-saturated conditions occurred at the surface so it is possible to investigate the role of melting and sublimation of ice hydrometeors. Finally, detailed measurements on the height and width of the transition have been conducted along Fortress Mountain (FOR) using the 'car-sonde' technique described in Thériault et al. (2018).

On 31 March 2015, a weather event associated with a rain-snow boundary along the mountainside occurred in the Kananaskis Valley. The sounding launched at 2100 UTC shows sub-saturated conditions near the surface at the KES site (Fig. 2). The MMR2 reflectivity profiles (Fig. 3a) show precipitation reaching the surface for about 2 hours. The bright band is located at the level where solid precipitation started to melt (Fig. 3a). Measurements along FOR using the 'car-sonde' technique indicated that the top of the rain-snow boundary was at 1750 m ASL. The rain-snow transition is located about 200 m below the 0°C isotherm, which confirms the presence of a non-melting layer just above the level where the wet-bulb temperature, T_w, is 0°C, as discussed in Harder and Pomeroy (2013).

The surface temperature at 2100 UTC 31 March 2015 varies from 12°C to 3°C whereas the dew point temperature increases up to the onset of precipitation (Fig. 3b). Wind speed is generally weak throughout the precipitation event, with variable directions (Fig. 3c). Manual observations at the KES site show that light rain started at 2030 UTC 31 March 2015, changing
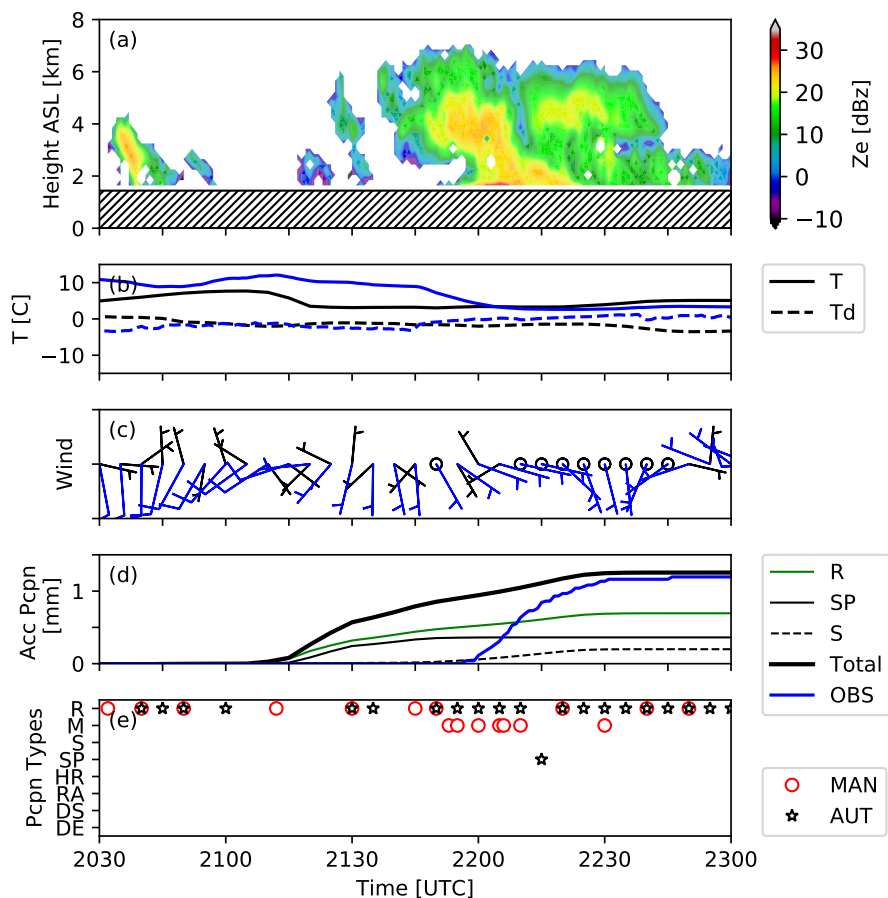
Figure 3. Atmospheric conditions and precipitation fields during the 31 March 2015 event at KES. (a) Reflectivity field measured by the Micro Rain Radar; (b) surface temperature (T) and dew point (Td) observed (blue line) and simulated (black line); (c) wind speed and direction using wind barbs, where the observed is blue and simulated is black; (d) unadjusted liquid equivalent accumulated precipitation observed (blue line, OBS) and simulated (bold black line for total, green line for rain, thin black line for snow pellets and dashed black line for snow), and (e) the type of precipitation observed manual (MAN) and automatically (AUT) at KES. These are rain (R), snow pellets (SP), snow (S), mixed precipitation (M), heavily rimed snow (HR), rimed aggregates (RA), dry snow (DS) and dendrites (DE). Simulated results are for the CTL run. Adapted from Thériault et al. (2018).

to a mixture of rain, snow and snow pellets, then to a brief period of only snow (Fig. 3e). This is supported by the automatic diagnostic of precipitation types using the Ishizaka et al. (2013) method also used in Thériault et al. (2018).

3 Description of the simulations

3.1 Model configuration

The simulations are performed using the Weather Research and Forecasting (WRF) model, version 3.7.1 (Skamarock and Klemp, 2008). Three-dimensional (3D) simulations are used with initial and boundary conditions provided by the North American Regional Reanalysis (NARR) data from the National Center for Environmental Prediction (NCEP) (Mesinger et al., 2006). Two-way nesting with four nested grids (27 km, 9 km, 3 km and 1 km) is used to perform high-resolution simulations over the Kananaskis valley. The high-resolution domain is shown in Fig. 1. The control run and the sensitivity tests are conducted with the two-moment bulk microphysics scheme of Milbrandt and Yau (2005a, b) to predict cloud and precipitation.

Other parameterizations used in the simulations includes the Rapid Radiative Transfer Model (RRTMG) with the Monte Carlo Independent Column Approximation (MCICA) method of random cloud overlap scheme (Iacono et al., 2008) for longwave and shortwave radiation. Also, the Noah Land Surface Model (Tewari et al., 2004) with soil temperature and moisture in four layers, fractional snow cover and frozen soil physics is used. The planetary boundary layer is parameterized in the simulations with the Yonsei University scheme, which uses the non-local K approach with an explicit entrainment layer and a parabolic K profile in the unstable mixed layer, where K is the vertical diffusion coefficient (Hong et al., 2006). Cumulus parameterization is used on the coarser grid only (27 km) with the Kain-Fritsch scheme (Kain, 2004).

To have the maximum number of vertical levels within the melting layer, 56 vertical levels are used where the grid spacing varies from 50 to 320 m in the first 2 km and is between 320 m and 340 at higher levels. The simulation on the coarser grids (27, 9 and 3 km) starts at 1500 UTC 31 March 2015, 3 hours prior to the higher resolution grid (1 km), which starts at 1800 UTC 31 March 2015. The simulations are integrated for a total of, 12 h and 9 h, respectively. The time step used is 90 s on the coarser grid (27 km) decreasing with a ratio of 3 between each nested grid to 3.33 s on the higher resolution grid (1 km).

3.2 Description of the microphysics scheme and modifications

The two-moment microphysics scheme predicts the mass mixing ratio and the total number concentration of inverse exponential size distribution of six hydrometeor categories: cloud droplets, rain, ice crystals, snow, graupel (i.e. snow pellets in this study), and hail. Each category is described by an assumed mass-diameter relationship and an associated fall speed. The evolution of clouds and precipitation is based on many microphysical processes that are mainly divided into cold and warm processes in the microphysics scheme. In this study we focus on the sublimation and melting of ice particles as well as on the formation of snow pellets. This last process includes the collision/coalescence of ice crystals and snow with cloud droplets or raindrops leading to rimed particles. A detail description of all processes is given in Milbrandt and Yau (2005a, b). Since the area of interest for this study is located in a sub-saturated environment, the scheme is modified to allow snow to sublimate at all temperatures. In the original Milbrandt and Yau (2005a, b) two-moment scheme, snow sublimation can only occur when the temperature is below 0°C, while snow pellets can sublimate at all temperatures. Some modifications were made to this original scheme (Poirier, 2017). First, the sublimation rate equation was updated so that snow and snow pellets can sublimate at all

(c) Author(s) 2019. CC BY 4.0 License.

temperatures. Second, the calculation of saturation vapour pressure was adjusted to accurately compute the sublimation rate at all temperatures (Poirier, 2017).

3.3 Description of the sensitivity experiments

The control simulation (CTL) is conducted using the modified microphysics and model configuration described in section 3.1
and 3.2. To estimate the impact of temperature changes from melting and sublimation, first, a sensitivity simulation is run while neglecting the latent heating/cooling due to the melting of snow and snow pellets (MLT). A second sensitivity simulation is performed, in a similar manner, on the impact of temperature changes from sublimation of solid precipitation (SBL). Because accreted particles were often observed during the field campaign, a last sensitivity simulation is performed without snow pellet formation (SNP) to assess the type and intensity rate of precipitation that would reach the surface without riming aloft.

The data are analyzed in a systematic manner. First, the CTL simulation is compared to available observations such as wind speed and direction, temperature, relative humidity, height of the rain-snow transition as well as precipitation amount and types collected during the field project. The time evolution of mass-mixing ratio of ice crystals, cloud, rain, snow pellets and snow are analyzed at the grid point closest to the KES site. To analyse precipitation aloft at KES and in the Kananaskis Valley, a vertical cross section is plotted and the mass mixing ratio of hydrometeors as well as the vertical air motion are investigated.
Second, the CTL simulation is compared to the three sensitivity experiments: the simulation without the temperature change from melting of snow and snow pellets (MELT), the simulation without the temperature change from sublimation (SBL) and the simulation without snow pellets (SNP). Finally, the impact of wind direction and precipitation types formed aloft on the precipitation amounts and types reaching the surface is investigated.

4 Comparison between observations and the control simulation

The CTL simulation is compared to observations to ensure that atmospheric conditions are well reproduced by the model. First, the simulated liquid equivalent accumulated precipitation is compared to observations in Fig. 4. Comparison shows agreement at KES and NAK but an overestimation by the model near FOR. The gradient of precipitation along the mountainside is well-represented, showing that rain accumulated in the valley. In summary, both observations and CTL simulation show that the precipitation amount accumulated at KES is relatively low during this event and dominated by rain with a higher accumulation of snow produced at high elevations (Fig. 4).

Concerning the general meteorological parameters, the CTL run reproduces the observations at KES well (cf. Fig. 3). First, the simulated and observed dew point are similar, whereas the temperature is different before the onset of precipitation but reaches similar values during the precipitation event (cf. Fig. 3b). The wind direction is highly variable but both the simulation and observation have southerly components before the onset of precipitation while the simulations exhibit slightly stronger winds (<5 knots) during the event (cf. Fig. 3c). Solid precipitation is simulated at temperatures >0°C in the Kananaskis area as reported during the field project. Precipitation amounts simulated at KES are very low and reach 1.3 mm during the event in agreement with observations (Fig. 3d). The rain-snow boundary occurred at warmer temperatures than if the environmental
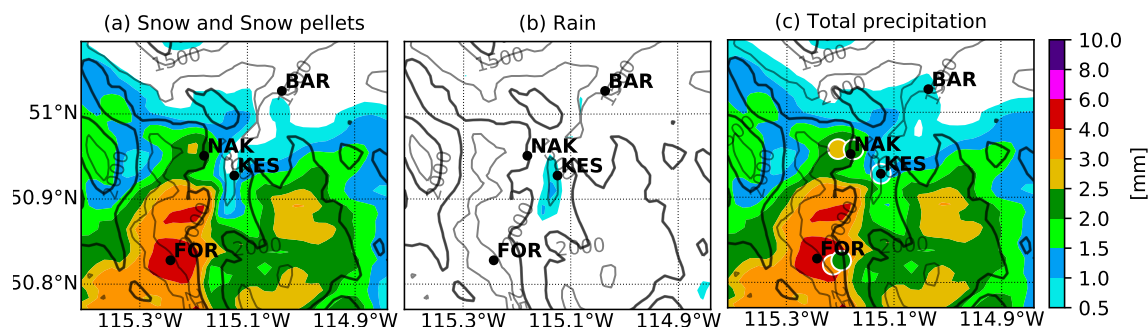
Figure 4. Simulated (a) unadjusted accumulated solid precipitation (mm) including snow and snow pellets, (b) rain and (c) total accumulated precipitation between 2000 UTC 31 March 2015 and 0000 UTC 1 April 2015. The coloured circles in (c) are the observations at 5 locations. Accumulated precipitation is in liquid equivalent.

conditions were saturated, and is reproduced between 2100 and 2230 UTC 31 March 2015, as observed. The simulated height of the melting layer (Fig. 5a-d) corresponds to the same as measured by the MRR2 (Fig. 3a). The comparison of Fig. 3d and 3e shows an agreement between the type of hydrometeors simulated and observed, with the predominance of rain and the presence of snow pellets.

5   The vertical structure of hydrometeors at KES is also investigated. The riming of ice crystals with cloud droplets at 6 km ASL is a minor source of snow pellets (Fig. 5a-c). The main source of snow pellets seems to be riming of snow with cloud droplets based on the order of magnitude mixing ratio of both snow and snow pellets (Fig. 5b-d). Snow occurs aloft throughout the event, but only reaches the surface from 2145 UTC until 2230 UTC at a precipitation rate of ∼0.5 mm/h as it sublimates before reaching the surface (Fig. 5d). Rain occurs simultaneously with snow pellets and snow at the surface throughout the

10   event (Fig. 5e). It corresponds mainly to the type of precipitation reported in Fig. 3e.

The vertical cross-section of hydrometeors when snow starts to reach the surface (2145 UTC) is shown in Fig. 6 across the Kananaskis valley. The maximum mass-mixing ratios of ice crystals and cloud droplets aloft occurred on the windward side of the mountains (Fig. 6a and b) and are transported across the valley. The location of the maximum amount of ice crystals corresponds to the elevation where snow is formed. At that level, ice crystals interact with cloud droplets to produce snow

15   pellets aloft (Fig. 6c). Snow is transported eastward by the wind and sublimates (Fig. 6d). The upward air motion leads to the formation of ice crystals (Fig. 6a) and cloud droplets (Fig. 6b) aloft above the westward barrier, which are converted into snow and snow pellets and transported downstream (Fig. 6c and d). Clouds (both ice and liquid) and precipitation produced on the westward barrier (-10 km) are transported east of KES.

In summary, the weather conditions at KES are generally well represented by the model during the precipitation event.

20   The remaining analysis will focus on the microphysical processes near KES. In particular, the impact of sublimation and the occurrence of snow pellets on the formation and evolution of precipitation types and amounts, as well as the wind field are investigated.
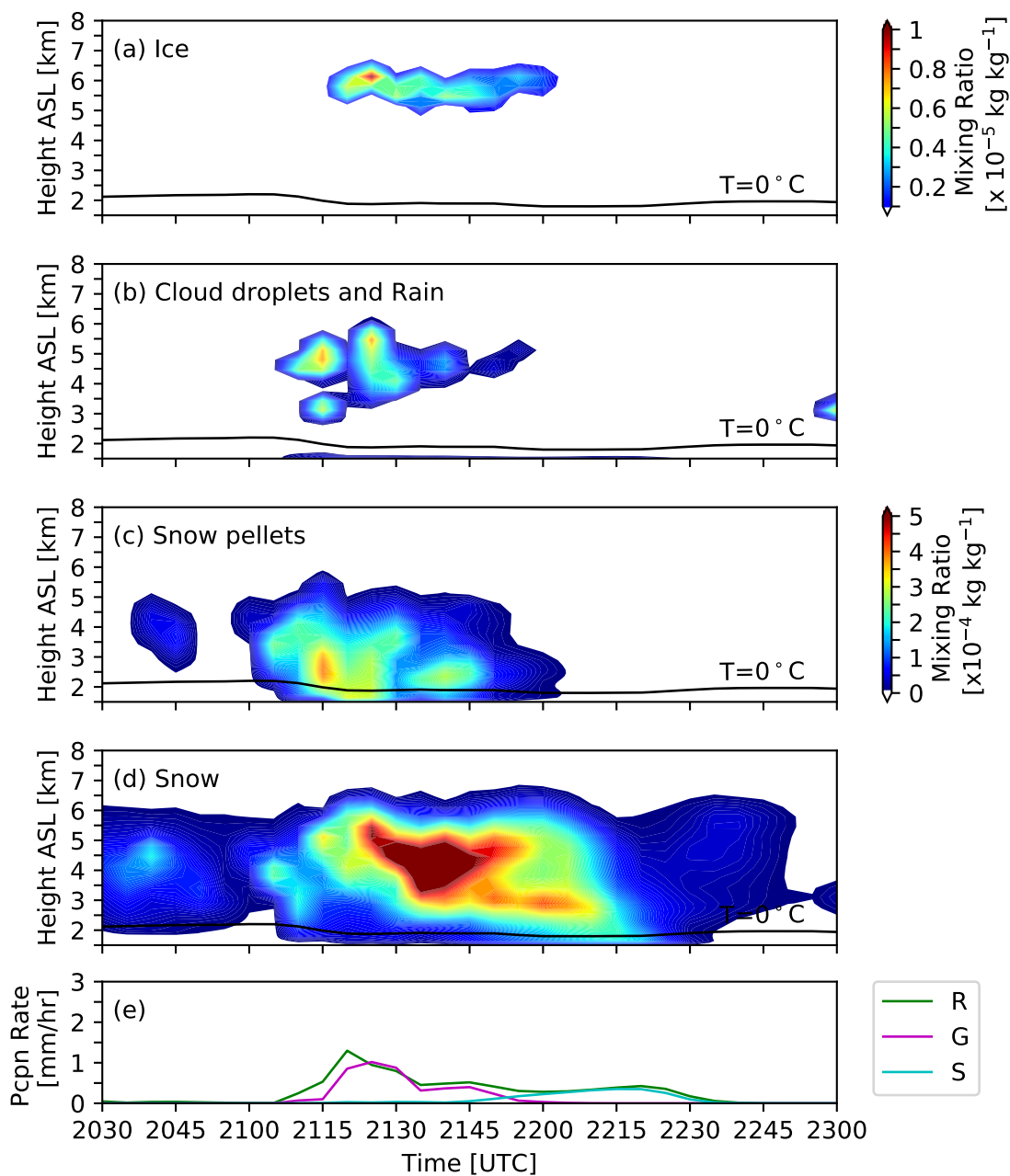
Figure 5. CTL simulation: times series at KES of the mass-mixing ratio of (a) ice crystals, (b) cloud droplets and rain, (c) snow pellets, (d) snow and (e) the surface precipitation rate of rain (R), snow pellets (G) and snow (S). The 0°C isotherm is indicated by the solid black line on (a), (b), (c) and (d). Panels b-d have the same colour scale.
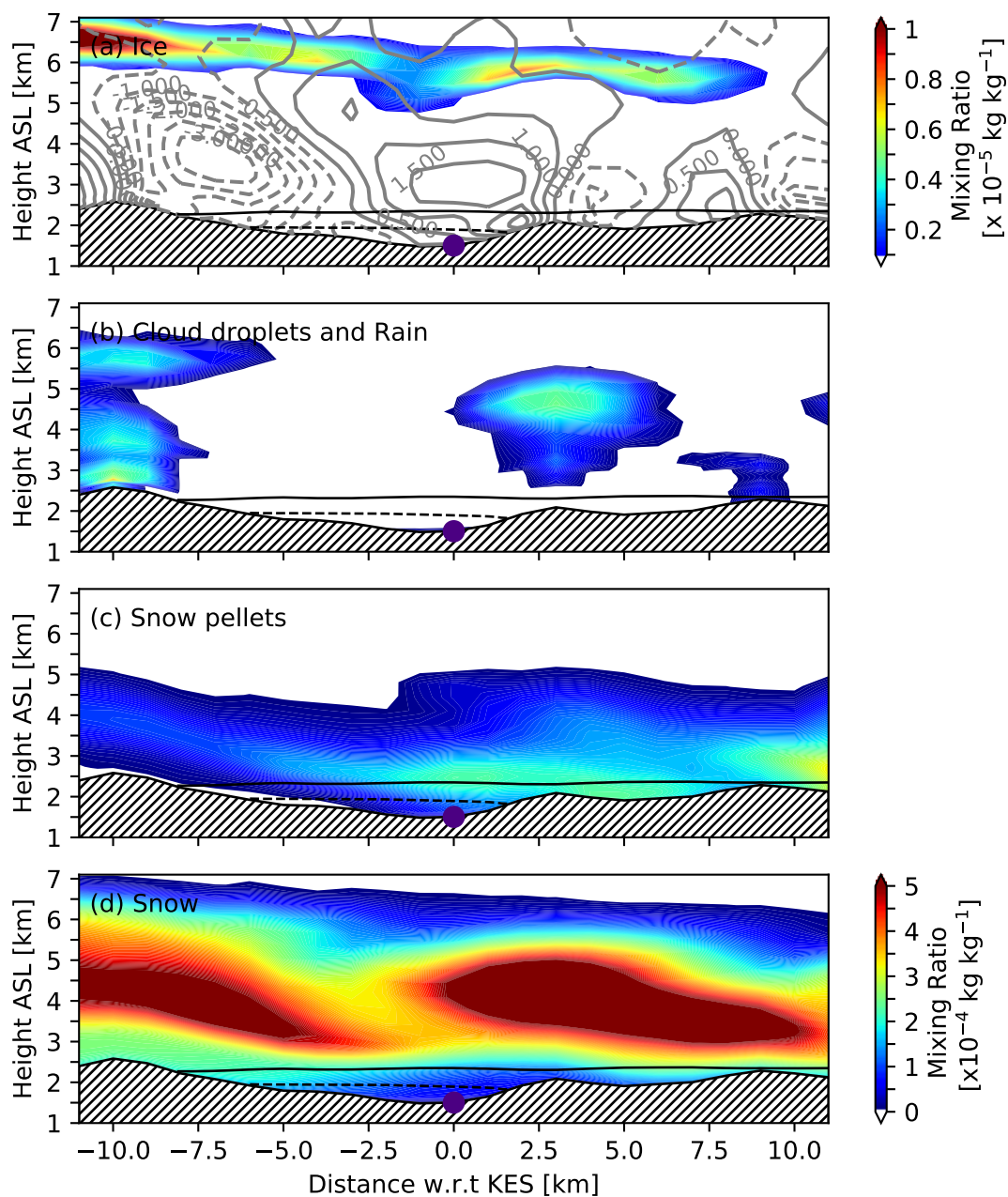
Figure 6. CTL simulation: vertical cross section across the Kananaskis Valley showing the mass-mixing ratio of (a) ice crystals, (b) cloud droplets and rain, (c) snow pellets, (d) snow at 2145 UTC. The location of KES is indicated by the black dot. The shaded area indicates the topography. The 0°C isotherm is indicated by the solid black line and the 0°C wet bulb temperature is the black dashed line. (a) includes vertical air motion (m/s), as well. Panels b to d have the same colour scale.
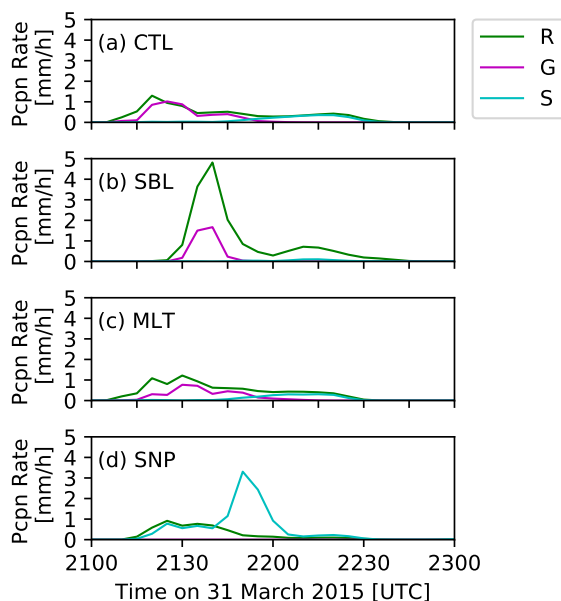
Figure 7. Precipitation rates at KES produced by (a) the control simulation (CTL), (b) the simulation without cooling from sublimation (SBL) and (c) melting (MLT) as well as the simulations without the production of snow pellets (SNP).

5 Hydrometeor evolution during the event: CTL versus sensitivity experiments

The role of phase changes and of the production of snow pellets on precipitation amounts and types reaching the surface at KES are investigated. The CTL simulation is compared with a series of sensitivity experiments (no temperature change from melting of solid hydrometeors i.e. MLT; no temperature change from sublimation of solid hydrometeors i.e. SBL; no snow

5 pellets formation i.e. SNP). First, for MLT, differences with CTL on the surface precipitation intensity and type at KES are minor (Fig. 7a and c). For example, MLT simulation produces slightly less precipitation than CTL, but the precipitation types and their evolution is similar (Fig. 7a and 7c). In contrast, the evolution of precipitation intensity and types varies significantly at KES, in comparison with CTL for SBL and SNP (Fig. 7b and 7d). The peak in precipitation occurred at the beginning of the event (∼2135 UTC) in the warmer environment (SBL) and later during the event (∼2150 UTC) when no snow pellets were

10 produced (SNP). Given these findings, the effects of temperature changes from sublimation and riming on the production and the evolution of precipitation are further investigated.

The time series of the vertical evolution of clouds and precipitation for the CTL and the sensitivity experiments at KES is shown in Fig. 8. The edge contour of the hydrometeor is indicated to illustrate the relative location of clouds and precipitation using a mass-mixing ratio minimum threshold value of 10^{-6} kg/kg. The distribution of hydrometeors at KES when no cooling

15 from melting (MLT) is considered produces a similar precipitation and cloud distribution as the CTL (Fig. 8a and c). When no temperature change from sublimation is considered (SBL), the timing of precipitation is delayed in comparison to CTL (Fig. 8a and b). In that case, the ice and liquid water clouds persist for a longer time period than CTL. Moreover, the top of the

ice cloud extends up to 7 km leading to snow pellet formation at higher elevations compared to CTL (Fig. 8a and b). In SBL, the elevation of the 0°C isotherm is higher than CTL because the environmental air is generally warmer (Fig. 8a and b). It produces favourable conditions for solid precipitation to melt into rain before reaching the surface. These statements suggests a link among the maximum precipitation rate at the surface produced in warmer conditions (SBL, Fig. 7b) as well the highest

5 ice crystal mass-mixing ratio aloft (not shown). For SNP, ice crystals, cloud droplet and precipitation distribution aloft, as well as at the surface, differs from the CTL simulation (Fig. 8d and Fig. 7d). Less ice crystals and cloud droplets are produced aloft compared to CTL. This could be explained by the lack of warming from accretion resulting in colder temperatures, which leads to less ice nucleation aloft (e.g. Meyers et al., 1992). Below the ice cloud, less cloud droplets are produced for a similar reason. Once snow pellets are formed, the environmental temperature increases due to the latent heat of fusion from the freezing of

10 cloud droplets. As snow pellets fall through sub-saturated conditions, they cool the environment because of sublimation, which alters the distribution of hydrometeors aloft (Fig. 8a in comparison to Fig. 8d). Finally, in SNP, the peak in surface precipitation rate is delayed because only relatively slow-falling ice particles such as snowflakes are formed (Fig. 7d).

The vertical evolution of hydrometeors when snow starts to reach the surface in CTL (2145 UTC) across the Kananaskis Valley differs for each simulation (Fig. 9). First, for MLT, no significant difference is observed with CTL simulation for the

15 reason discussed earlier in this section (Fig. 9a and c). Second, for SBL, more rain reaches the surface in the valley because the environmental temperature is higher in comparison to CTL (Fig. 9a and b). For SBL, vertical air motions are stronger on the slope east of KES to produce a deep liquid water cloud (Fig. 9a and b). The ice cloud is also higher and deeper in SBL due to warmer conditions (Fig. 9b). The formation of snow pellets also affects the distribution of cloud and precipitation in the Kananaskis Valley (Fig. 9a and d). In SNP, the ice cloud extends up to KES but it does not interact with the liquid water cloud,

20 which is formed at lower levels compared to CTL (Fig. 9d). At this time, the snowfall rate at the surface increases rapidly to reach 3 mm/h and the rain rate decreases. From Fig. 8, the time series of hydrometeor evolution is completely different for SNP compared to other three cases studies. Therefore, the cross-section at 2145 UTC (Fig. 9d) is not representative of the precipitation onset but it corresponds to a time when the many types of hydrometeors are simulated aloft (Fig. 8d).

The following section will discuss the processes leading to the changes in clouds and precipitation distribution when no

25 temperature changes from sublimation and no snow pellets are produced. It assesses the role of sublimation and snow pellet formation on the vertical and horizontal evolution of precipitation intensity and types in the Kananaskis Valley.

6   Role of sublimation and snow pellet formation

Neglecting the cooling due to sublimation results in higher temperatures at both the surface and aloft (Fig. 10). This higher temperature aloft in the SBL run would increase the amount of snow aloft and at the surface but only aloft for snow pellets.

30 As, KES is located on the windward side of the Kananaskis Valley, there is generally upward motion at that location. The warmer conditions in SBL produce more instability and, in turn, stronger upward motion. This upward motion leads to thicker and higher ice clouds and liquid water clouds (Fig. 10b). Comparing CTL to SBL, (Figs. 7a, b) show that the maximum precipitation occurs at the beginning of the event for CTL. Warmer conditions in SBL delays the onset of precipitation because
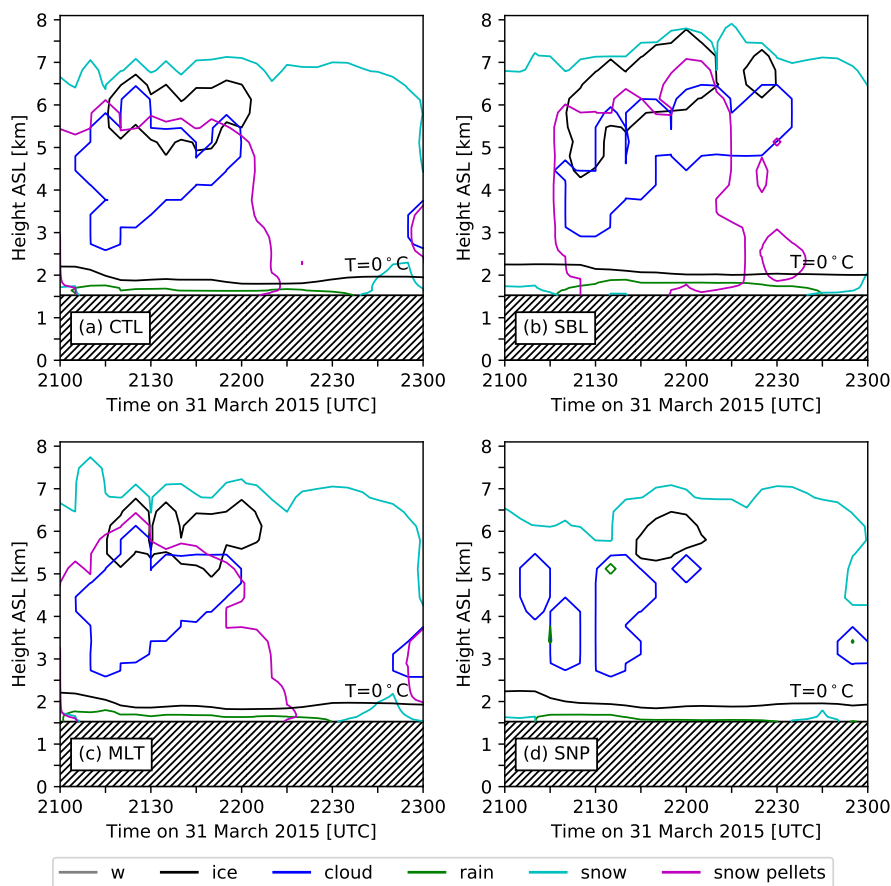
Figure 8. Vertical distribution of clouds and precipitation indicated by a mass-mixing ratio minimum threshold (10^{-6} kg/kg) at KES during the event for (a) CTL, (b) SBL, and (c) MLT as well as (d) SNP.

of sub-saturated conditions aloft. Once the clouds are formed, precipitation reaches the surface at higher rates at KES because less is being transported eastward. The higher rain rate is due to a higher melting level aloft allowing for complete melting of solid precipitation before reaching the ground.

   Snow pellets formation impacts the surface precipitation intensity and types, in particular, by indirectly influencing the wind
5 flow in the valley. For the CTL case, the evolution of the horizontal wind speed between the onset of the precipitation and the end of the precipitation event (Figs, 11a and b) shows that the direction and magnitude of the wind speed changes at the end of the precipitation event in the valley close to KES on the western slope. For the SNP, this flow reversal on the windward side of the mountain is suppressed (Fig. 11e and f) whereas it is maintained in SBL (Fig. 11c and d) and MELT (not shown) with a smaller magnitude in both cases. This suggests that the cooling from sublimation and/or melting of snow pellets produces
10 denser air that moves down the mountainside.
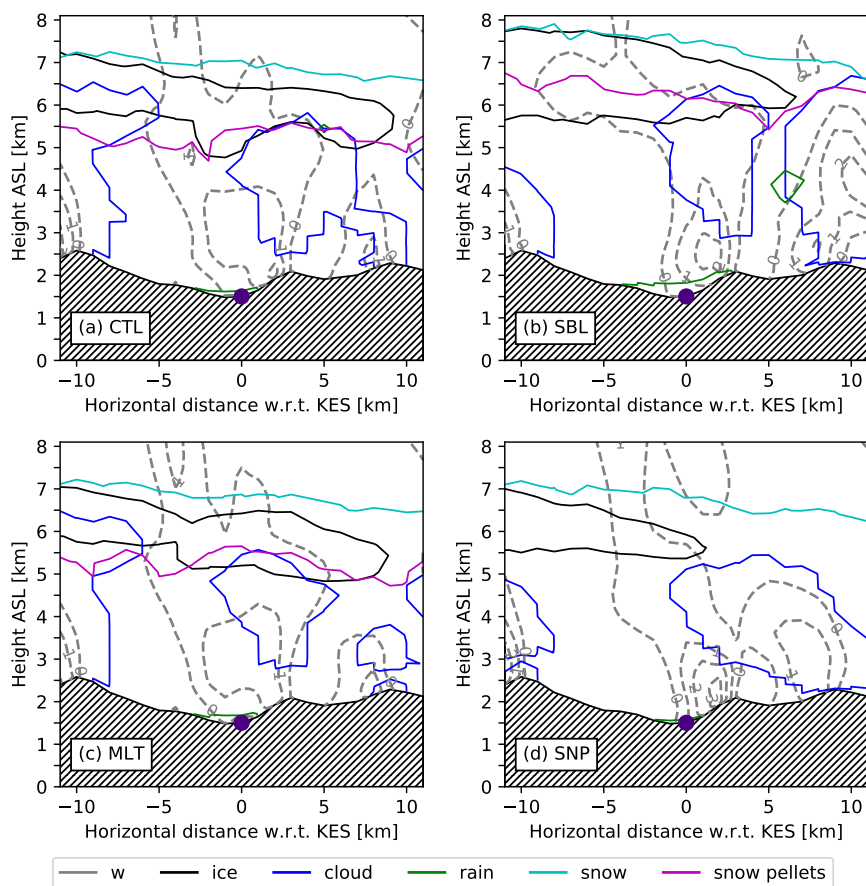
Figure 9. Vertical cross section across the Kananaskis Valley showing the distribution of cloud and precipitation indicated by a mass-mixing ratio minimum threshold similar to Fig. 8 at 2145 UTC for (a) CTL simulation, (b) SBL simulation, and (c) MLT simulation as well as (d) SNP simulation. The location of KES is indicated by the black dot. The grey dashed lines indicate the vertical wind. The shaded area is the topography.
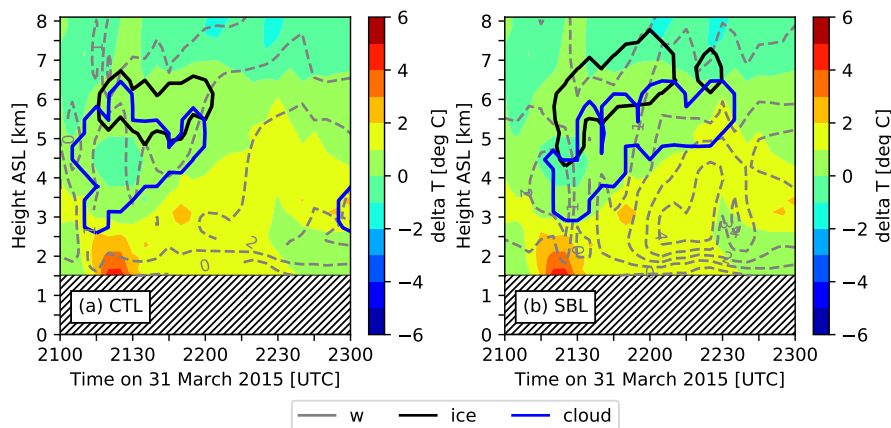
Figure 10. Time series of the vertical air motion (w, grey dashed lines) as well as the contour delimitating water and ice clouds using a minimum threshold of the mass-mixing ratio similar to Fig. 8 (blue, respectively, black line) are superimposed for (a) CTL and (b) SBL. The temperature difference between the SBL and the CTL simulations (delta T) is added to each panel.

In CTL and SNP, snow is produced mainly over the western barrier with respect to KES as shown on Figures 11a and b at the onset of precipitation. The snow mass-mixing ratio suggests that snow is transported downwind between the onset and end of the precipitation event (Fig. 11). The change in the zonal wind speed (Fig. 11a and c) prevents snow from falling at KES in CTL (Fig. 7a). As snowflakes fall at low speed (about 1 m/s), their trajectories are strongly dependant on the prevailing

5   horizontal wind field. Since easterly winds were up to 2 m/s at 2200 UTC in the CTL, very little snow reaches the surface at KES (Fig. 7a). In SNP, snow reaches the surface (Fig. 7d) because the downslope flow is weaker than in CTL. Note that in the warmer environment (SBL) the flow reversal is weaker than in the colder one (CTL) but stronger than without snow pellet formation (SNP). Hence, in the warmer environment (SBL), the deviation of the snow-mixing ratio is not as pronounced as in the colder environment. Furthermore, snowflakes are falling much more slowly than snow pellets (up to 4 times) and will

10 tend to more closely follow streamlines as than compared to snow pellets. This is a possible explanation for the difference in the surface precipitation intensity and types at KES (Fig. 7). Moreover, in SNP, less cloud droplets are produced (Fig. 8d) over KES. This is probably due to the lack of warming feedbacks from the production of snow pellets that is considered in CTL. Because, in SNP, less sublimation occurs above KES, the change in the valley flow field is not as strong as in CTL (Fig. 11). This leads to more orographic forcing in SNP, producing the clouds aloft. In this case, the amount of snow produced above

15 KES is negligible because snow produced aloft is advected downwind. Therefore, snow reaching KES is mainly formed on the western barrier with respect to KES. The precipitation is transported downwind to KES. This explains why the peak in precipitation rate occurs at later times near the end of the event for SNP (Fig. 7d). Finally, given that the trajectories of solid precipitation differ among SBL, CTL and SNP, the latent heating profiles also differ. The trajectories of precipitation particles can explain why more cooling from sublimation occurs in SNP than CTL. Snow would come from the western barrier and the
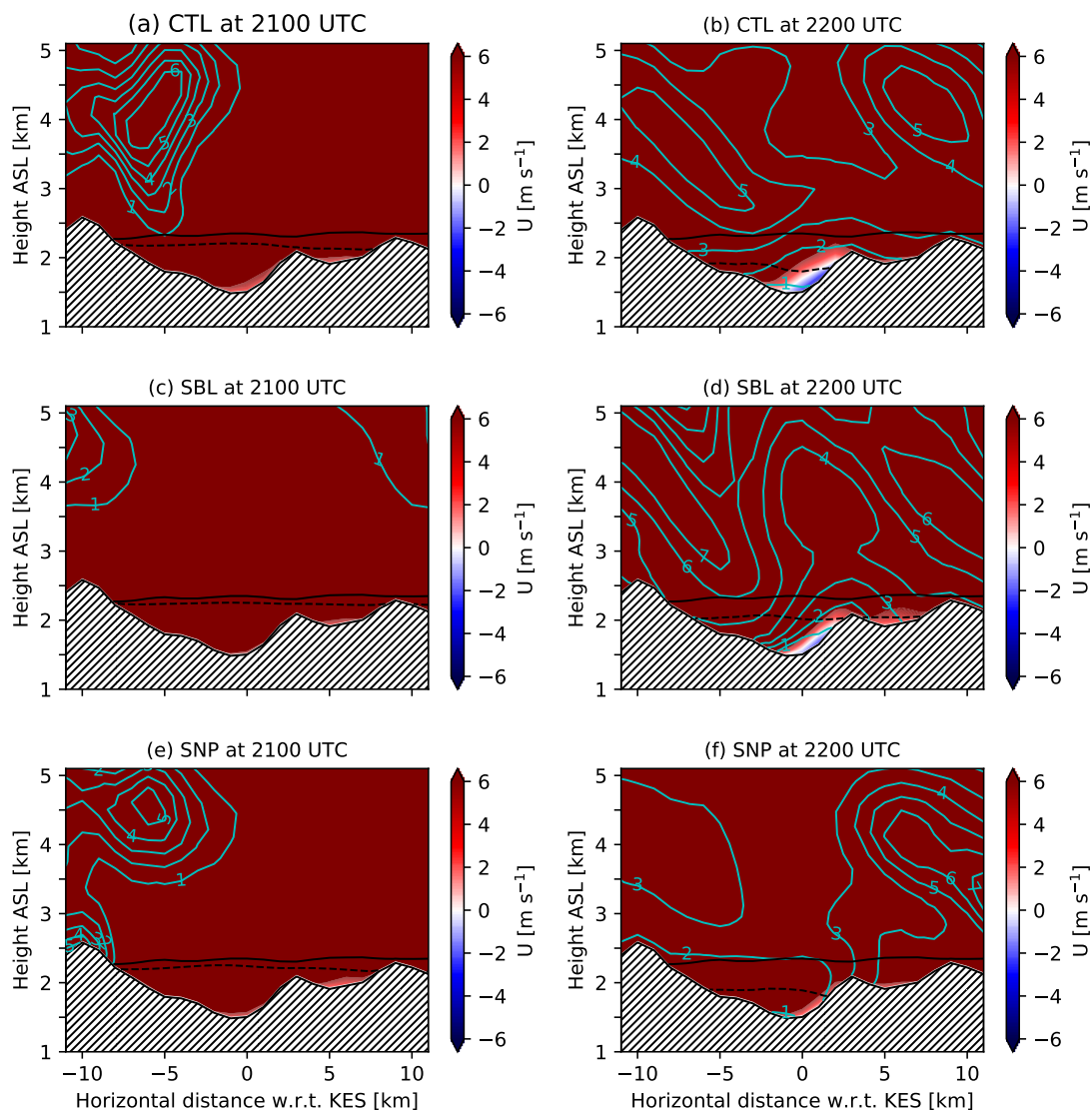
Figure 11. Vertical cross section across the Kananaskis Valley showing the snow field (10-4 kg/kg blue lines) and zonal wind speed (colour shading) at 2100 UTC (a, c, e) and 2200 UTC (b, d, f) for (a, b) CTL simulation, (b, c) SBL simulation and (e, f) SNP simulation. The black line indicates the location of the 0°C isotherm at the onset of precipitation and the black dashed line is the 0°C isotherm at the time of the analysis (2100 UTC and 2200 UTC). The shaded area is the topography. The negative (positive) wind speed values are easterly (westerly) winds.
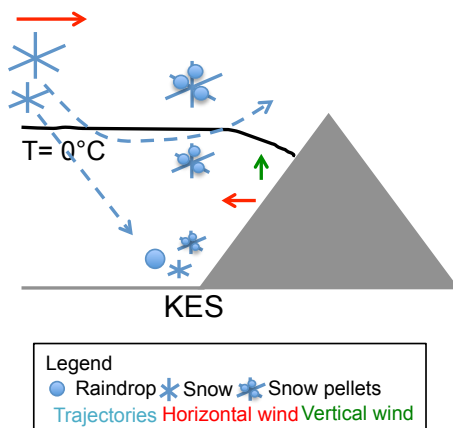
Figure 12. Conceptual model explaining the processes driving the evolution of precipitation in the Kananaskis Valley, Alberta. The black solid line is the 0°C isotherm. The grey area is the terrain.

sublimation would occur along the trajectories while simulations with faster falling particles, would lead to sublimation aloft in the Kananaskis Valley, closer to KES.

7 Summary and Conclusions

7.1 Summary

During the Alberta Field Project (Thériault et al., 2018), snow was often observed at surface temperatures above 0°C at the KES observation site. In general, precipitation occurred during relatively dry conditions. For example, solid precipitation was reported at the surface at temperatures up to 9°C with a relative humidity of 45%. Also, 60% of the particles observed were rimed (Hung, 2017). Given these findings, the relative impact of sublimation and melting of hydrometeors, as well as the role of snow pellets formation has been investigated. These are addressed by simulating a precipitation event associated with rain and mixed precipitation at the surface, which occurred on 31 March 2015, using the Weather and Research Forecasting (WRF) model.

Based on the simulations, a conceptual model explaining the processes leading to the observed precipitation distribution at KES is proposed in Fig. 12. The temperature variations from phase changes impacted the precipitation type, intensity and its temporal evolution at the surface. The warm conditions of this observed event led to unstable air and resulted in weak upward motion over a deeper layer. This produced a deep and high ice cloud with liquid water clouds below it. Snow pellets formed at the top of the liquid cloud and fell rapidly to the surface. At the same time, snowflakes were produced but were transported eastward. When crossing the Kananaskis Valley, snow particles are transported upward upstream of KES due to downslope flow. This downslope flow is mainly due to the cold and dense air produced by sublimation. The orographic forcing during the precipitation is weaker because of the strength of the downslope wind.

7.2 Conclusions

Based on the results obtained from the simulations and the conceptual model, key conclusions are as follows.

– the model reproduces well the atmospheric conditions and the precipitation amounts and type.

– Sublimation has a greater impact than melting on the evolution of the precipitation at the surface. This is due to the sub-saturated conditions in the lower atmosphere, which decreases the atmospheric layer where solid precipitation can melt.

– When the thermodynamic impact of sublimation is not considered, it alters the environmental temperature aloft. The warmer conditions create more upward motion, which leads to favourable conditions for accretion (snow pellets formation) aloft. Furthermore, it allows for a warmer melting layer near the surface resulting in a higher proportion of rain.

– As the precipitation falls and is transported by the wind, it alters the distribution of latent heating due to phase changes and, this, in turn, affects the wind direction along the mountainside.

– The trajectories of particles explain some of the differences in the precipitation amounts and types distribution at KES. Because snowflakes fall slower than snow pellets, they tend to more closely follow streamlines. For example, snow reaching the surface at KES is produced on the westward side of the Kananaskis Valley.

– The relative amount of snow reaching KES depends on the strength of the vertical wind shear above KES. Stronger down valley flow will tend to prevent snow particles to reach KES.

This study has some limitations. First, due to some instrumentation issues, the measurements of wind speed and wind direction during the Alberta Field Project were sometimes inconsistent. Second, this study also has some numerical limitations due to the choice of microphysics parameterization in the WRF model as well as the use of shallow convection parameterization at intermediate simulations. Different microphysics schemes would produce different precipitation rates and thus affect the cooling rate associated with sublimation and melting. Third, simulations using a particle-tracking model could be used to compute the trajectories of the precipitation particles to better assess the environmental conditions in which they fall.

Overall, this study shows that the microphysical processes leading to precipitation in complex terrain could significantly impact the precipitation intensity and type in the valley. Even if the study is conducted based on a relatively light precipitation event, critical scientific insights on the formation and evolution of precipitation are gained. Accurate representation of precipitation phase changes and accretion leading to snow pellets, as well as the wind field are critical, in particular in sub-saturated orographic regions such as the eastern slopes of the Canadian Rockies.

Data availability. The dataset used to conduct this study is available upon request to the corresponding author (Julie M. Thériault).These are the Weather and Research Forecasting (WRF) simulations, the necessary information and files to conduct the simulations and the simulations.

Competing interests. No competing interests are present.

Acknowledgements. We would like to thank the Natural Sciences and Engineering Research Council of Canada (NSERC) through the Discovery Grant and the Changing cold regions network (CCRN) as well as Global Water Futures for providing the financial support to accomplish this work. One of the authors (Émilie Poirier) would like to thank the Fond Quebecois de la recherche sur la nature et les

5 technologies (FRQNT) and NSERC for graduate scholarships.

References

Barth, M. C. and Parsons, D. B.: Microphysical processes associated with intense frontal rainbands and the effect of evaporation and melting on frontal dynamics, J. Atmos. Sci., 53, 1569–1586, 1996.

Battaglia, A., Rustemeier, E., Tokay, A., Blahak, U., and Simmer, C.: PARSIVEL snow observations: A critical assessment, J. Atmos. Oceanic Technol., 27, 333–344, 2010.

Burford, J. and Stewart, R. E.: The sublimation of falling snow over the Mackenzie River Basin, Atmos. Res., 49, 289–314, 1998.

Clough, S. A. and Franks, R. A. A.: The evaporation of frontal and other stratiform precipitation, Quart. J. Roy. Meteor. Soc., 117, 1057–1080, 1991.

Fargey, S., Hanesiak, J., Stewart, R., and Wolde, M.: Aircraft observations of orographic cloud and precipitation features over southern Baffin Island, Nunavut, Canada, Atmos. Ocean, 52, 54–76, 2014.

Harder, P. and Pomeroy, J.: Estimating precipitation phase using a psychrometric energy balance method, Hydrol. Process., 27, 1901–1914, 2013.

Henson, W., Stewart, R., and Hudak, D.: Vertical reflectivity profiles of precipitation over Iqaluit, Nunavut during Autumn 2007, Atmos. Res., 99, 217–229, 2011.

Hong, S.-Y., Noh, Y., and Dudhia, J.: A new vertical ciffusion package with an explicit treatment of entrainment processes, Mon. Wea. Rev., 134, 2318–2341, 2006.

Hung, I.: Characteristics and formation of precipitation over the kananaskis characteristics and formation of precipitation over the Kananaskis Emergency Site during March and April 2015, Master's thesis, University of Manitoba, 2017.

Iacono, M. J., Delamere, J. S., Mlawer, E. J., Shephard, M. W., Clough, S. A., and Collins, W. D.: Radiative forcing by long-lived greenhouse gases: Calculations with the AER radiative transfer models, J. Geophys. Res.: Atmos., 113, D13 103, 2008.

Ishizaka, M., Motoyoshi, H., Nakai, S., Shiina, T., Kumakura, T., and Muramoto, K.: A new method for identifying the main type of solid hydrometeors contributing to snowfall from measured size-fall speed relationship, J. Meteor. Soc. Jpn., 91, 747–762, 2013.

Kain, J. S.: The Kain–Fritsch convective parameterization: An update, J. Appl. Meteor., 43, 170–181, 2004.

Liu, A. Q., Mooney, C., Szeto, K., Thériault, J. M., Kochtubajda, B., Stewart, R. E., Boodoo, S., Goodson, R., Li, Y., and Pomeroy, J.: The June 2013 Alberta catastrophic flooding event: Part 1—Climatological aspects and hydrometeorological features, Hydrol. Process., 30, 4899–4916, 2016.

Marwitz, J. D.: The kinematics of orographic rirflow during Sierra Storms, J. Atmos. Sci., 40, 1218–1227, 1983.

Marwitz, J. D.: Deep Orographic Storms over the Sierra Nevada. Part I: Thermodynamic and Kinematic Structure, J. Atmos. Sci., 44, 159–173, 1987.

Matsuo, T., Sasyo, Y., and Sato, T.: Relationship between types of precipitation on the ground and surface meteorological elements, J. Meteorol. Soc. Jpn., 59, 462–476, 1981.

Mesinger, F., DiMego, G., Kalnay, E., Mitchell, K., Shafran, P. C., Ebisuzaki, W., Jović, D., Woollen, J., Rogers, E., Berbery, E. H., Ek, M. B., Fan, Y., Grumbine, R., Higgins, W., Li, H., Lin, Y., Manikin, G., Parrish, D., and Shi, W.: North American Regional Reanalysis, Bull. Amer. Meteor. Soc., 87, 343–360, 2006.

Meyers, M. P., DeMott, P. J., and Cotton, W. R.: New primary ice-nucleation paramterizations in an explicit cloud model, J. Climate. Appl. Meteor., 31, 708–721, 1992.

Milbrandt, J. A. and Yau, M. K.: A multi-moment bulk microphysics parameterization. Part I: Analysis of the role of the spectral shape parameter, J. Atmos. Sci., 62, 2051–3064, 2005a.

Milbrandt, J. a. and Yau, M. K.: A Multimoment Bulk Microphysics Parameterization. Part II: A Proposed Three-Moment Closure and Scheme Description, J. Atmos. Sci., 62, 3065–3081, 2005b.

5 Milrad, S. M., Gyakum, J. R., and Atallah, E. H.: A meteorological analysis of the 2013 Alberta flood: Antecedent large-scale flow pattern and synoptic-dynamic characteristics, Mon. Wea. Rev., 143, 2817–2841, 2015.

Minder, J. R., Durran, D. R., and Roe, G. H.: Mesoscale controls on the mountainside snow line, J. Atmos. Sci., 68, 2107–2127, 2011.

Parker, D. J. and Thorpe, A. J.: The role of snow sublimation in frontogenesis, Quart. J. Roy. Meteor. Soc., 121, 763–782, 1995.

Poirier, E.: Étude de la ligne pluie-neige dans la vallée de Kananaskis, Alberta, Master's thesis, Universite du Quebec a Montreal, 2017.

10 Pomeroy, J. W., Stewart, R. E., and Whitfield, P. H.: The 2013 flood event in the South Saskatchewan and Elk River basins: Causes, assessment and damages, Can. Water Resour. J., 41, 105–117, 2016.

Skamarock, W. C. and Klemp, J. B.: A time-split nonhydrostatic atmospheric model for weather research and forecasting applications, J. Comput. Phys., 227, 3465–3485, 2008.

Steiner, M., Bousquet, O., Houze Jr, R. a., Smull, B. F., and Mancini, M.: Airflow within major Alpine river valleys under heavy rainfall, Q. 15 J. Roy. Meteorol. Soc., 129, 411–431, 2003.

Stewart, R. E., Burford, J. E., Hudak, D. R., Currie, B., Kochtubajda, B., Rodriguez, P., and Liu, J.: Weather systems occurring over Fort Simpson, Northwest Territories, Canada, during three seasons of 1998–1999: 2. Precipitation features, J. Geophys. Res., 109, 1–19, 2004.

Tewari, M., Chen, F., Wang, W., Dudhia, J., LeMone, M., Mitchell, K., Ek, M., Gayno, G., Wegiel, J., and Cuenca, R.: Implementation and verification of the unified NOAH land surface model in the WRF model, in: 20th conference on weather analysis and forecasting/16th 20 conference on numerical weather prediction, pp. 11–15, 2004.

Thériault, J. M., Rasmussen, R., Smith, T., Mo, R., Milbrandt, J. A., Brugman, M. M., Joe, P., Isaac, G. A., Mailhot, J., and Denis, B.: A case study of processes impacting precipitation phase and intensity during the Vancouver 2010 Winter Olympics, Wea. Forecasting, 27, 1301–1325, 2012.

Thériault, J. M., Rasmussen, K. L., Fisico, T., Stewart, R. E., Joe, P., Gultepe, I., Clément, M., and Isaac, G. a.: Weather observations on 25 Whistler Mountain during five storms, Pure Appl. Geophys., 171, 129–155, 2014.

Thériault, J. M., Milbrandt, J. A., Doyle, J., Minder, J. R., Thompson, G., Sarkadi, N., and Geresdi, I.: Impact of melting snow on the valley flow field and precipitation phase transition, Atmos. Res., 156, 111–124, 2015.

Thériault, J. M., Hung, I., Vaquer, P., Stewart, R. E., and Pomeroy, J. W.: Precipitation characteristics and associated weather conditions on the eastern slopes of the Canadian Rockies during March–April 2015, Hydrology and Earth System Sciences, 22, 4491–4512, 2018.

30 Zängl, G.: Reversed flow in the south-Alpine Toce Valley during MAP-IOP 8: Further analysis of latent cooling effects, Quart. J. Roy. Meteor. Soc., 133, 1717–1729, 2007.